Biochemical and Biophysical Research Communications 454 (2014) 71–77

Contents lists available at ScienceDirect

Biochemical and Biophysical Research Communications

journal homepage: www.elsevier.com/locate/ybbrc

RBP-J-interacting and tubulin-associated protein induces apoptosis and cell cycle arrest in human hepatocellular carcinoma by activating the p53–Fbxw7 pathway

Haihe Wang [a], Zhanchun Yang [b], Chunbo Liu [a], Shishun Huang [a], Hongzhi Wang [a], Yingli Chen [a], Guofu Chen [b,*]

[a] The Key Laboratory of Molecular Diagnosis in Laboratory Medicine, Department of Pathogenobiology, Daqing Branch of Harbin Medical University, Daqing 163319, China
[b] Department of General Surgery of Fifth Clinical Hospital of Harbin Medical University, Daqing 163319, China

ARTICLE INFO

Article history:
Received 4 October 2014
Available online 14 October 2014

Keywords:
RITA
HCC
Notch signaling
Cell cycle arrest
Apoptosis

ABSTRACT

Aberrant Notch signaling is observed in human hepatocellular carcinoma (HCC) and has been associated with the modulation of cell growth. However, the role of Notch signaling in HCC and its underlying mechanism remain elusive. RBP-J-interacting and tubulin-associated (RITA) mediates the nuclear export of RBP-J to tubulin fibers and downregulates Notch-mediated transcription. In this study, we found that RITA overexpression increased protein expression of p53 and Fbxw7 and downregulated the expression of cyclin D1, cyclin E, CDK2, Hes-1 and NF-κB p65. These changes led to growth inhibition and induced G0/G1 cell cycle arrest and apoptosis in SMMC7721 and HepG2 cells. Our findings indicate that RITA exerts tumor-suppressive effects in hepatocarcinogenesis through induction of G0/G1 cell cycle arrest and apoptosis and suggest a therapeutic application of RITA in HCC.

© 2014 Elsevier Inc. All rights reserved.

1. Introduction

Hepatocellular carcinoma (HCC) accounts for 80–90% of liver cancers and is one of the most prevalent carcinomas throughout the world [1]. It is a common cancer and is occurring with increasing frequency in China. Epidemiological studies have revealed that cirrhosis with hepatitis virus infection is the most predominant risk factor for HCC development [2]; however, the exact molecular mechanism underlying HCC development has not been fully elucidated.

Many molecules and signaling pathways have been found to be involved in the development of HCC, including the CDKN1C/P57, Cyclooxygenase-2/Snail/E-cadherin, TGF-β, NF-κB, Bcl-2 [3–6], AKT/mTOR, RAF/MEK/ERK, EGFR and HGF/cMET pathways [7,8]. However, the mechanisms underlying the disruption of these critical pathways in the tumorigenesis of HCC are still not fully elucidated. The Notch signaling pathway may be important both for normal bile duct formation and abnormal neovascularization [9]. Studies have shown that Notch1, Notch4 and Jagged1 are upregulated in HCC [10,11] and that Notch promotes the progression of HCC. In contrast, others have shown that Notch1 signaling can significantly inhibit *in vitro* and *in vivo* growth of the HCC cell line SMMC7721 [12]. The transcription factor RBP-J may play an important role in the regulation of Notch signaling, as it is crucial for recognition of the DNA target sequences in both the repressor and activator complexes. RBP-J-interacting and tubulin-associated (RITA; C12ORF52) is a highly conserved, 36-kDa protein that has no significant homology to any other protein [13]. On a functional level, RITA interferes with Notch- and RBP-J-mediated transcription. RITA is subject to rapid shuttling between nucleus and cytoplasm, and most importantly, it mediates the nuclear export of RBP-J to tubulin fibers. RITA, as a novel RBP-J-interacting protein, downregulates Notch signaling by interfering with the transcription factor RBP-J.

In the present study, We have demonstrated that RITA upregulation can significantly inhibit the *in vitro* growth of the HCC cell line SMMC7721 and HepG2. Conversely, RITA knockdown promoted proliferation in the same cell line. RITA-induced growth suppression is at least partially due to G0/G1 cell cycle arrest and apoptosis. Consistent with cell cycle arrest, expression levels of cyclin D1, cyclin E, and CDK2 protein all decreased. Upregulation of p53 and Fbxw7 expression and downregulation of NF-κB p65 and Hes-1 were observed and may be related to RITA-induced apoptosis.

* Corresponding author.
E-mail address: zhangyanjie3@aliyun.com (G. Chen).

http://dx.doi.org/10.1016/j.bbrc.2014.10.023
0006-291X/© 2014 Elsevier Inc. All rights reserved.

2. Materials and methods

2.1. Cell culture and transfections

SMMC7721 and HepG2 cells were cultured in Dulbecco's modified Eagle's medium (DMEM) supplemented with 10% fetal calf serum at 37 °C and 5% CO_2. The intracellular domain of RITA (corresponding to base pairs 469–1279 of the full-length human RITA cDNA) was cloned into the pcDNA3.1/Flag (-)B vector to generate the Flag-tagged expression vector pcDNA3.1-Flag-RITA (GenePharma, Shanghai, China). RITA or mock vectors were transfected into SMMC7721 and HepG2 cells at 70% confluence using X-tremeGENE HP DNA transfection reagent (Roche, Mannheim, Germany) according to the manufacturer's protocol. Cells were transfected for 48 h in 6-well plates containing 2.5×10^5 cells per well and then analyzed for flow cytometry, MTT assay, Western blot and qRT-PCR.

2.2. RNA interference (RNAi)

RITA and control siRNAs were chemically synthesized (GenePharma, Shanghai, China), and the target sequences were designed according to Wacker et al. [13]. The siRNAs were delivered into the SMMC7721 and HepG2 cells at 70% confluence using X-tremeGENE siRNA transfection reagent (Roche, Mannheim, Germany) following the manufacturer's protocol. Cells were transfected for 48 h and then analyzed for different parameters.

2.3. Analysis of cell cycle and apoptosis

The cell cycle and apoptosis were analyzed by flow cytometry. After transfection with the corresponding siRNAs or RITA vectors, 1×10^6 cells were harvested and washed twice with cold PBS, then fixed in 75% alcohol for 2 h at 4 °C. After washing in cold PBS 3 times, cells were resuspended in 1 mL of PBS solution with 40 μg of propidium iodide (Sigma) and 100 μg of RNase A (Sigma) for 30 min at 37 °C and analyzed with the BD Accuri C6 system (Becton Dickinson, USA). The distribution of cells in different phases of the cell cycle was calculated using the Modifit LT software.

For the analysis of apoptosis, 1×10^6 cells were harvested and washed three times with cold PBS. Cells were then resuspended in the staining buffer and stained using the Annexin V-FITC Apoptosis Assay Kit (Bestbio, Shanghai, China) according to the manufacturer's instructions. The stained cells were analyzed by flow cytometry (BD FACSAria, R&D, USA). Annexin V-positive and propidium iodide-negative cells were counted as apoptotic cells.

2.4. Analysis of cell growth in vitro

Cell viability was assessed using the MTT colorimetric assay (R&D, USA). SMMC7721 and HepG2 cells were seeded in 96-well plates at a density of 1×10^4 cells per well in 100 μL complete medium. After transfection with the corresponding vector or siRNA, 10 μL MTT solution (5 mg/mL) was added, and cells were incubated for an additional 4 h. Next, 100 μL of MTT solubilization buffer was added to the wells. Following a 10-min mixing period, the absorbance was analyzed at 570 nm using a microplate reader. The background absorbance at 690 nm was subtracted from the 570 nm measurement. Each experiment was performed in triplicate, and the mean value was calculated.

2.5. Real-time quantitative reverse transcriptase polymerase chain reaction (qRT-PCR)

qRT-PCR was performed to quantify and validate RITA, p53, Fbxw7, NF-κB p65, Hes-1, cyclin A, cyclin D1, cyclin E and CDK2 mRNA expression, and GAPDH was used as a reference gene. The relative target mRNA levels were determined using the $2^{\Delta\Delta Ct}$ method. The primer sequences used are summarized in Table 1. PCR amplification was performed in 20 μL reactions containing cDNA generated from 2 ng of the original RNA template, 400 nmol/L of each gene-specific forward and reverse primer, 10 μL of 2× SYBR® Premix Ex Taq™ II (Takara, Dalian, China), 0.4 μL of ROX reference dye, and 6.0 μL of dH_2O. Amplified signals were detected using the ABI PRISM 7300 Real-Time PCR system (ABI, USA). Experiments were performed in duplicate.

2.6. Immunoprecipitation

Immunoprecipitation experiments were carried out using whole-cell extracts from SMMC7721 cells 24 h after cotransfection with RITA-Flag [13]. The extracts were incubated with 20 μL protein A/G-agarose beads (Shang Hai Yue-ke Biotechnology CO., LTD) at 4 °C for 4 h. After centrifugation, the supernatants were incubated with 100 μL anti-Flag rabbit antibody (1:100) (M2, Sigma) or 100 μL anti-RBP-J mouse antibody (1:100) (Institute of Immunology Co., Ltd), respectively at 4 °C for 60 min. Non-immune rabbit IgG was also used as a control at the step. Then 50 μL protein A/G-agarose beads were added and incubated for 2 h at 4 °C. The beads were washed 6–8 times with PBS and resuspended in SDS–polyacrylamide gel loading buffer. Proteins were resolved by 10% SDS–PAGE and transferred to nitrocellulose (NC) membrane (Bio-Rad). The membranes were pre-blocked for 2 h at room temperature with TBS-T (0.1 M Tris, 0.9% NaCl, and 0.05% Tween-20 at pH 7.5) containing 5% skim milk. The following antibodies were used: anti-Flag (M5, Sigma; secondary antibody, GE healthcare), anti-RBP-J (rat monoclonal IgG2a, Institute of Immunology Co., Ltd.; secondary antibody peroxidase-conjugated goat anti-rat IgG, Dianova).

2.7. Western blot analysis

Protein concentrations were determined using the BCA Protein Assay (Pierce, USA), according to the manufacturer's instructions.

Table 1
Primer for PCR amplification and siRNAs sequences.

Sequencing primers	5′–3′
p53-F primer	CAGATCCCTTAGTTTTGGGTGC
p53-R primer	GCCTGGAGAGACCTAGACCA
Fbxw7-F primer	AAAGAGTTGTTAGCGGTTCTCG
Fbxw7-R primer	CCACATGGATACCATCAAACTG
HES-1-F primer	CCAAAGACAGCATCTGAGCA
HES-1-R primer	TCAGCTGGCTCAGACTTTCA
NF-κB-F primer	TCTGCAACTGAAACGCAAGC
NF-κB-R primer	CTCCACAGCTTCTCTTACCTT
CDK2-F primer	CGGATCTTTCGGACTCTGGG
CDK2-R primer	GAGAGGGTGAGCCGATTAGG
CyclinA-F primer	CAGAGGCCGAAGACGAGAC
CyclinA-R primer	TCAGCTGGCTTCTTCTGAGC
CyclinD1-F primer	CTGGCCATGAACTACCTGGA
CyclinD1-R primer	GTCACACTTGATCACTCTCC
CyclinE-F primer	GTTATAAGGGAGACGGGGAG
CyclinE-R primer	TGCTCTGCTTCTTACCGCTC
RITA-F primer	GGGTGGAGAAGGCTAACAGAA
RITA-R primer	CATCACAGTAAGACGGGGTGT
GAPDH-F primer	AGGTGAAGGTCGGAGTCAAC
GAPDH-R primer	CGCTCCTGGAAGATGGTGAT
RITA-siRNA1-sense	GGCUAACAGAACCAGAGGCtt
RITA-siRNA1-antisense	GCCUCUGGUUCUGUUAGCCtt
RITA-siRNA2-sense	GGAAGAAGAACAAAUACAGtt
RITA-siRNA2-antisense	CUGUAUUUGUUCUUCUUCCtt
Control-siRNA-sense	UUCUCCGAACGUGUCACGUtt
Control-siRNA-antisense	ACGUGACACGUUCGGAGAAtt

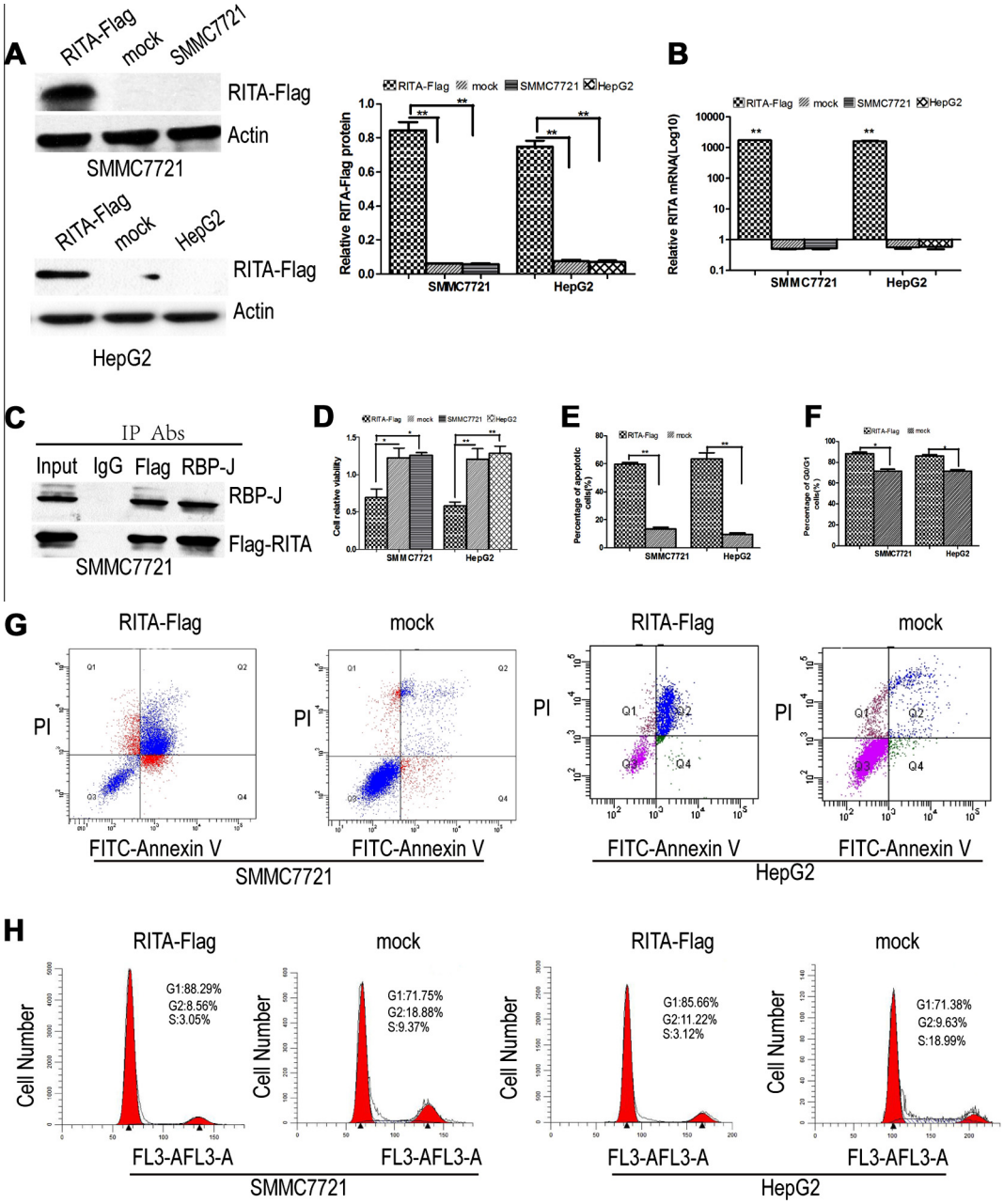

Fig. 1. Effects of RITA overexpression on SMMC7721 and HepG2 cells growth. (A and B) SMMC7721 and HepG2 cells were transfected with an expression vector containing RITA and empty vector (mock), or they were left untreated. (C) Endogenous RBP-J protein was coimmunoprecipitated with RITA proteins using the anti-Flag antibody and detected by an anti-RBP antibody. (D) Cell proliferation was quantified by MTT assay. SMMC7721/RITA and HepG2/RITA cells grew significantly more slowly than mock or untreated cells. (E and G) Apoptosis and cell cycle were monitored by flow cytometry. The percentage of early apoptotic cells was quantified, and the fraction of apoptotic SMMC7721/RITA and HepG2/RITA cells were higher than that of mock cells ($P < 0.05$). (F and H) SMMC7721/RITA and HepG2/RITA cells showed a higher proportion of cells in G0/G1 phase (88.29% and 85.66%) compared with control cells (71.75% and 71.38%) ($P \leqslant 0.05$).

Samples containing equal amounts of protein (40 μg) were resolved by 10% SDS–PAGE and transferred to nitrocellulose membranes. After blocking for 2 h at room temperature with TBS-T containing 5% skim milk, the membranes were probed with rabbit anti-Flag (1:400), rabbit anti-p53 (1:400), rabbit anti-Fbxw7 (1:400), rabbit anti-cyclin A (1:400), rabbit anti-cyclin D1 (1:400), rabbit anti-cyclin E (1:400), rabbit anti-CDK2 (1:400) (Beijing Biosynthesis Biotechnology Co, Beijing, China), rabbit anti-NF-κB p65 (1:2000), rabbit anti-Hes-1 (1:2000) (Cell Signaling Technology Inc., Boston, USA), and mouse anti-actin (1:8000). Proteins were detected by exposing the blots to X-ray film (Kodak).

2.8. Statistical analysis

SPSS version 17.0 software was used for all statistical analyses. All of the results are expressed as the mean ± SD. Statistical analysis was performed using standard 2-way ANOVA for repeated measurements, and the X^2 test was used to analyze the flow cytometry

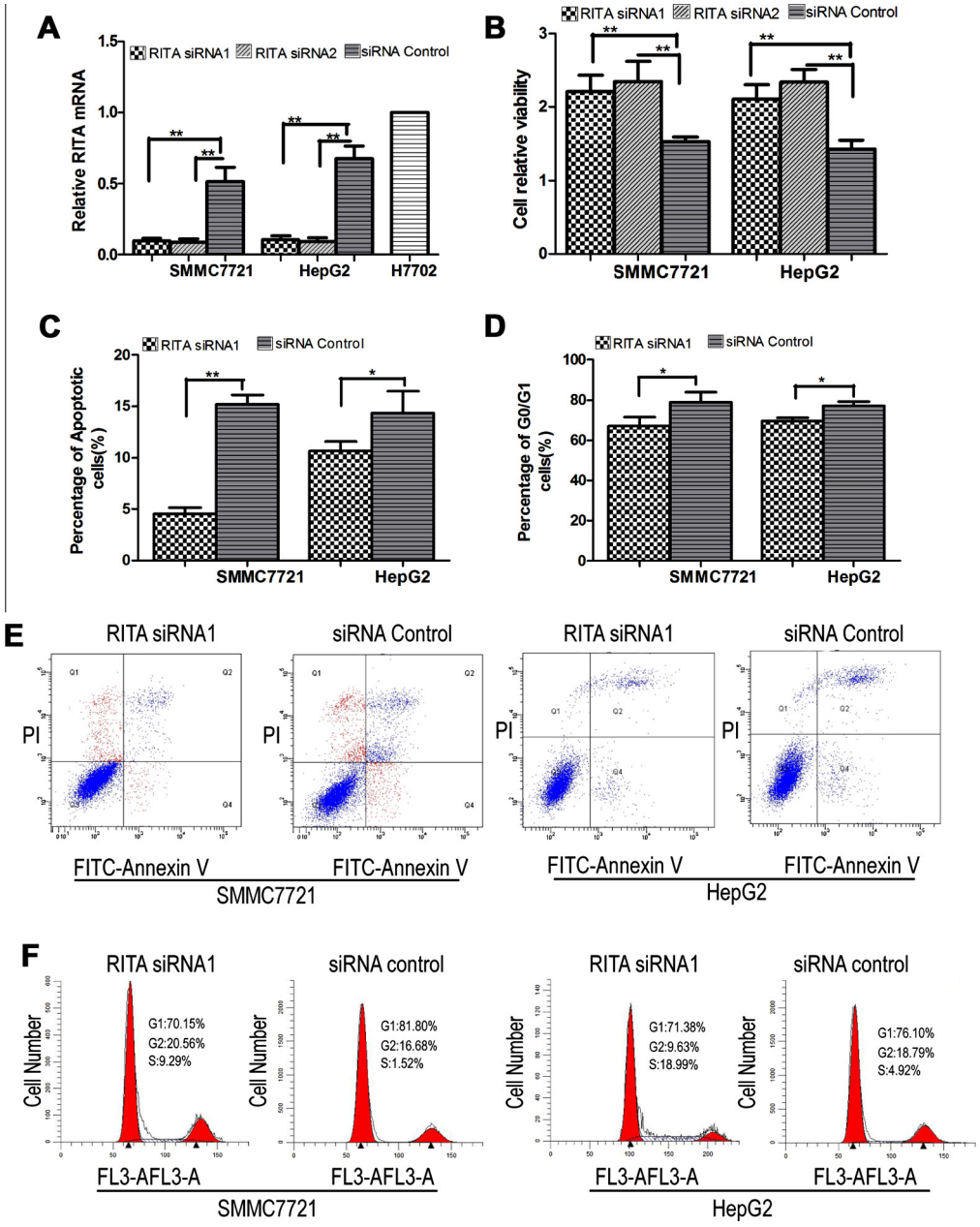

Fig. 2. Effects of RITA knockdown on SMMC7721 and HepG2 cells growth. (A) qRT-PCR was used to determine the relative mRNA expression of RITA in RITA siRNAs, control siRNA, SMMC7721, HepG2 and H7702 cells. GAPDH was used as an internal control. (B) Cell proliferation was quantified by MTT assay. RITA siRNA-transfected SMMC7721 and HepG2 cells grew significantly faster than control siRNA-transfected cells ($P < 0.05$). (C and E) Apoptosis was detected by flow cytometry. The percentage of early apoptotic cells was quantified, and the fraction of apoptotic cells was lower in RITA siRNA-transfected cells than in those transfected with control siRNA ($P < 0.05$). (D and F) RITA knockdown significantly increased the cell cycle progression. The percentage of G0/G1 phase in RITA siRNA cells (70.15% and 71.38%) was lower than that of control siRNA cells (81.80% and 76.10%) ($P \leqslant 0.05$).

data. P values less than 0.05 were considered statistically significant.

3. Results

3.1. RITA overexpression induces apoptosis and cell cycle arrest in SMMC7721 and HepG2 cells

The expression levels of RITA-Flag in SMMC7721/RITA and HepG2/RITA were assessed by qRT-PCR and Western blot assay. To examine the interaction between RITA and RBP-J, we performed immunoprecipitation experiments on a cellular background. Compared with the control, SMMC7721/RITA and HepG2/RITA cells showed higher expression of RITA-Flag (Fig. 1A and B). After incubation of lysates with an anti-Flag antibody, coimmunoprecipitated endogenous RBP-J proteins were detected using an anti-RBP-J antibody (Fig. 1C). The results of the MTT assay (Fig. 1D) indicate that overexpression of RITA caused growth inhibition in SMMC7721 and HepG2 cells. SMMC7721/RITA and HepG2/RITA grew significantly more slowly than mock vector-transfected cells (SMMC7721/pcDNA3.1 and HepG2/pcDNA3.1) or untreated cells ($P < 0.05$). We found that apoptosis was more prevalent in SMMC7721/RITA and HepG2/RITA cells than in mock vector-transfected cells ($P \leqslant 0.05$, Fig. 1E and G). Furthermore, flow cytometry

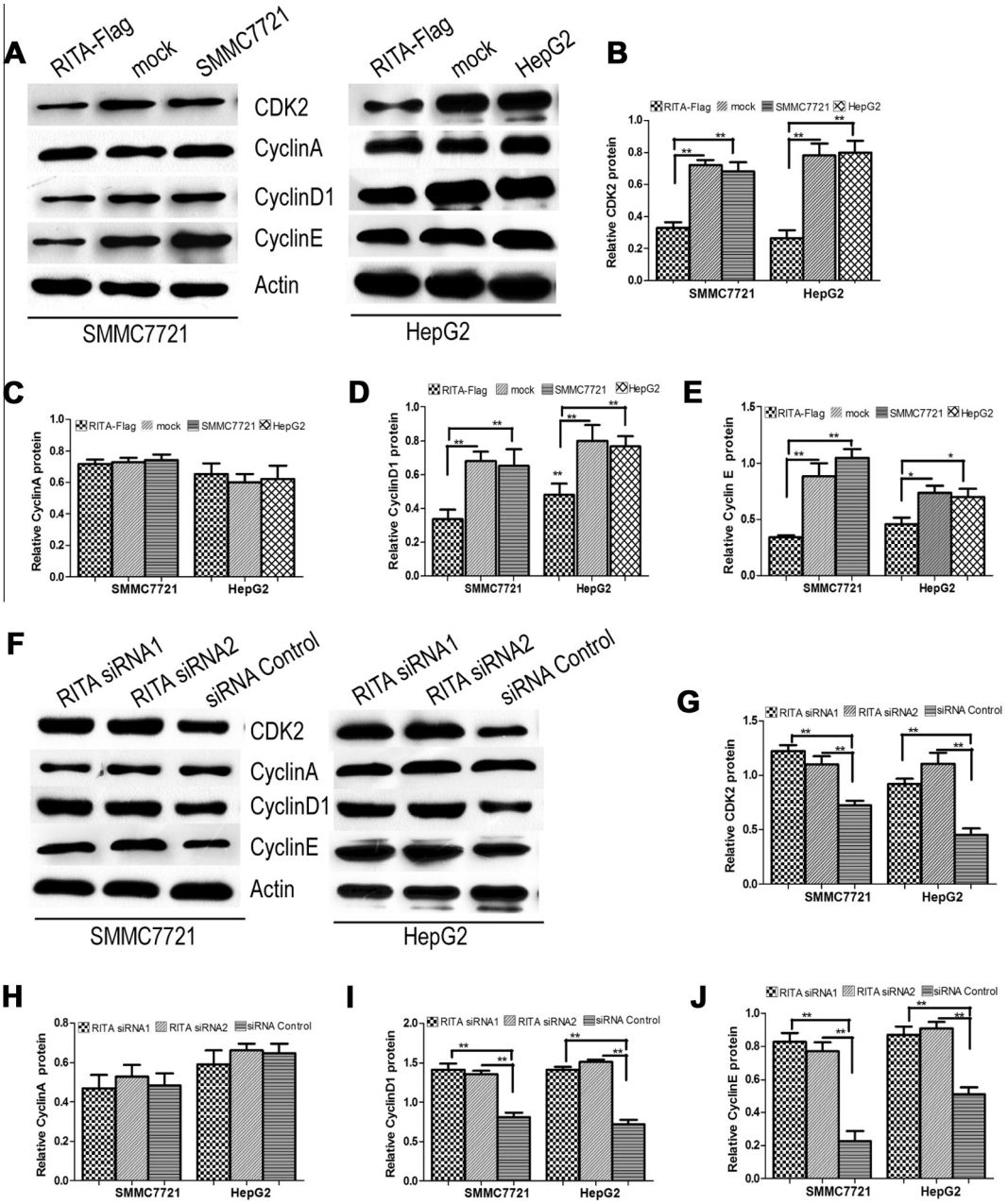

Fig. 3. Effect of RITA on CDK2, cyclin A, cyclin D1, and cyclin E. (A–E) Western blot was used to analyze cyclin A, cyclin D1, cyclin E, and CDK2 protein expression. Actin served as internal control. Cyclin D1, cyclin E, and CDK2 expression levels were significantly decreased in SMMC7721/RITA and HepG2/RITA cells compared to SMMC7721, HepG2 and mock cells ($P < 0.05$). (F–J) cyclin A, cyclin D1, cyclin E, and CDK2 protein were analyzed by Western blot in RITA siRNAs and control siRNA cells. CDK2, cyclin D1, and cyclin E expression levels were increased when compared with control siRNA-transfected cells ($P < 0.05$).

analysis was used to measure the cell cycle distribution in SMMC7721/RITA and HepG2/RITA cells. As predicted, SMMC7721/RITA and HepG2/RITA cells showed a higher proportion of cells in G0/G1 phase (88.29% and 85.66%) compared with control cells (71.75% and 71.38%) ($P \leqslant 0.05$, Fig. 1F and H).

3.2. Downregulation of RITA activates proliferation of SMMC7721 and HepG2 cells

To test siRNA efficiency, RITA transcript levels were evaluated by qRT-PCR. The level of RITA expression in RITA siRNA-transfected cells was reduced compared with control siRNA-transfected cells (Fig. 2A). Cell viability was evaluated using the MTT assay. The viability of transfected cells that expressed RITA siRNA was increased in comparison with cells that expressed control siRNA ($P < 0.05$, Fig. 2B). Flow cytometry analysis showed that RITA knockdown lowered the rate of apoptosis in SMMC7721 and HepG2 cells ($P \leqslant 0.05$, Fig. 2C and E) compared with control siRNA-transfected ($P < 0.05$). RITA knockdown significantly increased the cell cycle progression. The percentage of G0/G1 phase in SMMC7721 and HepG2 RITA siRNA cells (70.15% and 71.38%) was lower than that of control siRNA cells (81.80% and 76.10%) (Fig. 2D and F).

3.3. RITA down-regulates the expression of CDK2, cyclin D1, and cyclin E

Western blot analysis showed that 48 h after transient transfection with RITA-Flag, CDK2, cyclin D1, and cyclin E expression levels were significantly decreased ($P \leqslant 0.05$, Fig. 3A, B, D and E), but

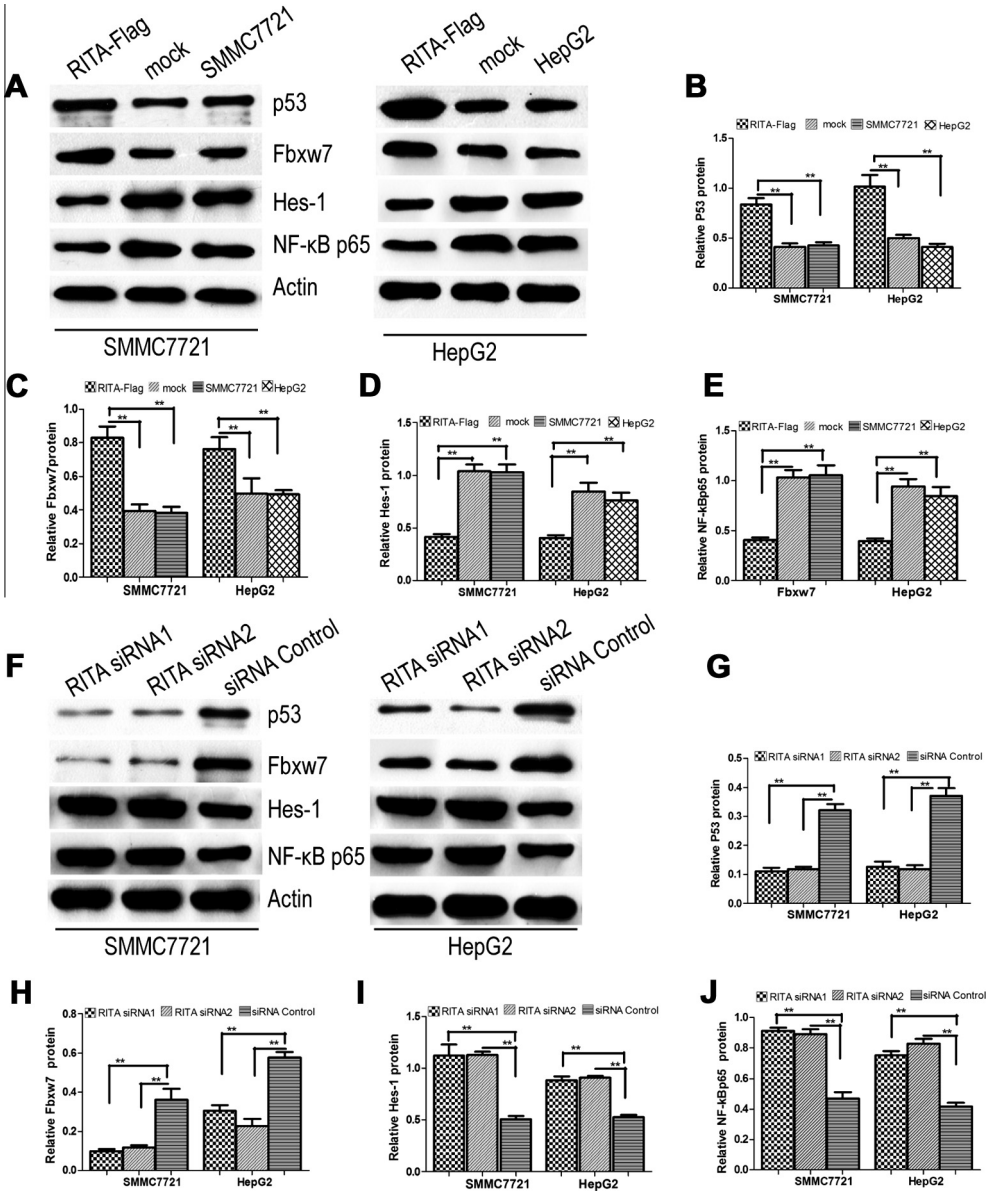

Fig. 4. Effect of RITA on p53, Fbxw7, Hes-1 and NF-κB p65. (A–E) Western blot was used to analyze p53, Fbxw7, Hes-1 and NF-κB p65 protein. Actin served as internal control. p53 and Fbxw7 were significantly increased, Hes-1 and NF-κB p65 were significantly decreased in SMMC7721/RITA and HepG2/RITA cells compared to SMMC7721, HepG2 and mock cells ($P < 0.05$). (F–J) showed p53, Fbxw7, Hes-1 and NF-κB p65 protein expression in RITA siRNAs and control siRNA cells. The protein of p53 and Fbxw7 were significantly decreased, Hes-1and NF-κB p65 were significantly increased in RITA siRNA cells compared to control siRNA cells ($P < 0.05$).

cyclin A exhibited no difference(Fig. 3C), when compared with SMMC7721 and HepG2 and mock cells. In contrast, CDK2, cyclin D1, and cyclin E expression levels were increased significantly 48 h after transient transfection with RITA siRNAs cells when compared with control siRNA-transfected cells ($P \leqslant 0.05$, Fig. 3F–J). The mRNA expression of these proteins were consistent with those obtained by Western blot (not shown).

3.4. RITA up-regulates the expression of p53, Fbxw7, and down-regulates Hes-1 and NF-κB p65

Western blot analysis showed that transient RITA-Flag induced a significant increase in p53 and Fbxw7 expression in SMMC7721 and HepG2 cells 48 h after transfection ($P \leqslant 0.05$, Fig. 4A–C), while the expression of Hes-1 and NF-κB p65 were significantly decreased compared with SMMC7721, HepG2 and mock cells, ($P \leqslant 0.05$, Fig. 4A, D and E). Forty-eight hours after RITA siRNA expression, Hes-1 and NF-κB p65 expression were increased (Fig. 4F, I and J), whereas p53 and Fbxw7 were down-regulated in RITA siRNA cells compared with control siRNA-transfected cells ($P \leqslant 0.05$, Fig. 4F–H). The mRNA expression of these proteins were similar with those obtained by Western blot (not shown).

4. Discussion

In this study, we employed several strategies to investigate the function of RITA in driving HCC development or progression. We transiently transfected Flag-tagged expression vectors of RITA and RITA-specific siRNA into SMMC7721 and HepG2 cells. We observed that RITA overexpression caused growth inhibition, induced G0/G1 cell cycle arrest and promoted apoptosis in SMMC7721 and HepG2 cells, whereas ablation of RITA improved viability. The role of the Notch cascade in HCC is controversial,

and despite strong data indicating that Notch activation facilitates tumor progression in the liver [14–17], some reports have suggested otherwise [12,18,19]. Aberrant Notch1 and Notch3 gene expression has been observed in HCC and has been associated with modulation of cell growth and response to chemotherapy. Studies have shown that Notch3 knockdown increased apoptosis and DNA damage in doxorubicin-treated HepG2 cells [12,20]. Other groups have found that Notch1, Notch3, Notch4, Jagged1, Delta1 and HES1 are all expressed in HepG2 cells [21–23]. Therefore, RITA may have caused growth inhibition in SMMC7721 cells by interfering with Notch- and RBP-J-mediated transcription.

Apoptosis and cell cycle arrest involve complex molecular pathways, and dysfunction of various genes may lead to the onset and progression of apoptosis and cell cycle arrest. We explored the mechanism of RITA-induced apoptosis and cell cycle arrest by assessing the effect of RITA on the expression of apoptosis-related factors (p53, Fbxw7, Hes-1, and NF-κB p65) and cell cycle regulators (cyclin A, cyclin D1, cyclin E, and CDK2) in SMMC7721 and HepG2 cells. Previous studies have demonstrated that overexpression of mutant or wild-type p53 can result in apoptotic cell death and that p53 can cause cell cycle arrest by transcriptionally upregulating p21 [24]. Fbxw7 is a key tumor suppressor that regulates cell proliferation in different HCC cell lines. It has been shown that Fbxw7 is directly regulated by p53 [25]. High levels of Fbxw7 might decrease the pool of available cell cycle regulators (cyclin E, cyclin A), triggering arrest in G1 phase and accounting for low proliferation rates. NF-κB signaling has been recognized as the major pathway responsible for cytokine-associated cancer development; inactivation of NF-κB inhibits cell growth and induces intrinsic apoptosis in hepatocellular carcinoma cells [26]. Protein levels and kinase activities of cyclin A, cyclin D1, cyclin E, and CDK4 are significantly elevated in HCC, and decreased levels of cyclin D1 have been correlated with growth inhibition and G0–G1 cell cycle arrest [27,28]. Here, we found a similar effect with RITA modulation in HCC cell lines. We showed that upon transient expression of active RITA in SMMC7721 and HepG2 cells, p53 and Fbxw7 expression levels were increased, whereas cyclin D1, cyclin E, CDK2, Hes-1 and NF-κB p65 were downregulated. RITA knockdown by siRNA caused downregulation of p53 and Fbxw7 and upregulation of cyclin D1, cyclin E, CDK2, Hes-1 and NF-κB p65. Taken together, our results suggest that Notch signaling can be inactivated by RITA, leading to increased protein expression of p53 and Fbxw7, and increased degradation of cyclin D1, cyclin E, CDK2, Hes-1 and NF-κB p65. RITA possibly induces G0–G1 cell cycle arrest through a mechanism of downregulating cyclin D1, cyclin E, CDK2, and Fbxw7 and synergizing with p53 to trigger apoptosis *in vitro*. To the best of our knowledge, our study provides the first evidence for RITA-induced G0/G1 cell cycle arrest and apoptosis in SMMC7721 and HepG2 cells.

In summary, our results show that RITA is a potential tumor marker that is involved with cell survival and growth of hepatocellular carcinoma cells. This suggests that RITA is deeply involved in the progression of hepatocellular carcinoma and may be a useful biomarker for the diagnosis and therapy of HCC.

Conflict of interest

None.

Acknowledgments

This work was supported by grants from Science and Technology Research Project of Education Department of Heilongjiang Province of China (Grant No. 12531271).

References

[1] Y.H. Kang, M.Y. Park, D.Y. Yoon, et al., Dysregulation of overexpressed IL-32α in hepatocellular carcinoma suppresses cell growth and induces apoptosis through inactivation of NF-κB and Bcl-2, Cancer Lett. 318 (2012) 226–233.
[2] K. Tu, X. Zheng, Z. Zhou, et al., Recombinant human adenovirus-p53 injection induced apoptosis in hepatocellular carcinoma cell lines mediated by p53-Fbxw7 pathway, which controls c-Myc and cyclin E, PLoS ONE 8 (2013) e68574.
[3] C. Giovannini, L. Gramantieri, M. Minguzzi, et al., CDKN1C/P57 is regulated by the Notch target gene Hes1 and induces senescence in human hepatocellular carcinoma, Am. J. Pathol. 181 (2012) 413–422.
[4] L. Zhou, D.S. Wang, Q.J. Li, et al., The down-regulation of Notch1 inhibits the invasion and migration of hepatocellular carcinoma cells by inactivating the cyclooxygenase-2/Snail/E-cadherin pathway in vitro, Dig. Dis. Sci. 58 (2013) 1016–1025.
[5] K. Wu, J. Ding, C. Chen, et al., Hepatic transforming growth factor beta gives rise to tumor-initiating cells and promotes liver cancer development, Hepatology 56 (2012) 2255–2267.
[6] A. Villanueva, C. Alsinet, K. Yanger, et al., Notch signaling is activated in human hepatocellular carcinoma and induces tumor formation in mice, Gastroenterology 143 (2012) 1660–1669.
[7] B. Blechacz, G.J. Gores, Tumor-specific marker genes for intrahepatic cholangiocarcinoma: utility and mechanistic insight, J. Hepatol. 49 (2008) 160–162.
[8] C. Ho, C. Wang, S. Mattu, et al., AKT (v-akt murine thymoma viral oncogene homolog 1) and N-Ras (neuroblastoma ras viral oncogene homolog) coactivation in the mouse liver promotes rapid carcinogenesis by way of mTOR (mammalian target of rapamycin complex 1), FOXM1 (forkhead box M1)/SKP2, and c-Myc pathways, Hepatology 55 (2012) 833–845.
[9] S.S. Nijjar, H.A. Crosby, L. Wallace, et al., Notch receptor expression in adult human liver: a possible role in bile duct formation and hepatic neovascularization, Hepatology 34 (2001) 1184–1192.
[10] C. Giovannini, L. Gramantieri, P. Chieco, et al., Selective ablation of Notch3 in HCC enhances doxorubicin's death promoting effect by a p53 dependent mechanism, J. Hepatol. 50 (2009) 969–979.
[11] S. Nishina, H. Shiraha, Y. Nakanishi, et al., Restored expression of the tumor suppressor gene RUNX3 reduces cancer stem cells in hepatocellular carcinoma by suppressing Jagged1-Notch signaling, Oncol. Rep. 26 (2011) 523–531.
[12] R. Kopan, M.X. Ilagan, The canonical Notch signaling pathway: unfolding the activation mechanism, Cell 137 (2009) 216–233.
[13] S.A. Wacker, C. Alvarado, G. von Wichert, et al., RITA, a novel modulator of Notch signalling, acts via nuclear export of RBP-J, EMBO J. 30 (2011) 43–56.
[14] M.T. Dill, L. Tornillo, T. Fritzius, et al., Constitutive Notch2 signaling induces hepatic tumors in mice, Hepatology 57 (2013) 1607–1619.
[15] D.F. Tschaharganeh, X. Chen, P. Latzko, et al., Yes-associated protein up-regulates Jagged-1 and activates the Notch pathway in human hepatocellular carcinoma, Gastroenterology 144 (2013) 1530–1542 (e12).
[16] S.O. Lim, Y.M. Park, H.S. Kim, et al., Notch1 differentially regulates oncogenesis by wildtype p53 overexpression and p53 mutation in grade III hepatocellular carcinoma, Hepatology 53 (2011) 1352–1362.
[17] M. Liu, D.F. Lee, C.T. Chen, et al., IKKα activation of NOTCH links tumorigenesis via FOXA2 suppression, Mol. Cell 45 (2012) 171–184.
[18] P. Viatour, U. Ehmer, L.A. Saddic, et al., Notch signaling inhibits hepatocellular carcinoma following inactivation of the RB pathway, J. Exp. Med. 208 (2011) 1963–1976.
[19] C. Wang, R. Qi, N. Li, et al., Notch1 signaling sensitizes tumor necrosis factor-related apoptosis-inducing ligand-induced apoptosis in human hepatocellular carcinoma cells by inhibiting Akt/Hdm2-mediated p53 degradation and up-regulating p53-dependent DR5 expression, J. Biol. Chem. 284 (2009) 16183–16190.
[20] D.M. Flynn, S. Nijjar, S.G. Hubscher, et al., The role of Notch receptor expression in bile duct development and diseases, J. Pathol. 204 (2004) 55–64.
[21] C. Giovannini, M. Lacchini, L. Gramantieri, et al., Notch3 intracellular domain accumulates in HepG2 cell line, Anticancer Res. 26 (2006) 2123–2127.
[22] J. Gao, C. Chen, L. Hong, et al., Expression of Jagged1 and its association with hepatitis B virus X protein in hepatocellular carcinoma, Biochem. Biophys. Res. Commun. 356 (2007) 341–347.
[23] J. Gao, Z. Song, Y. Chen, et al., Deregulated expression of Notch receptors in human hepatocellular carcinoma, Dig. Liver Dis. 40 (2008) 114–121.
[24] J.L. Roh, S.K. Kang, I. Minn, et al., P53-reactivating small molecules induce apoptosis and enhance chemotherapeutic cytotoxicity in head and neck squamous cell carcinoma, Oral Oncol. 47 (2011) 8–15.
[25] K. Tu, X. Zheng, G. Yin, et al., Evaluation of Fbxw7 expression and its correlation with expression of SREBP-1 in a mouse model of NAFLD, Mol. Med. Rep. 6 (2012) 525–530.
[26] V. Baud, M. Karin, Is NF-kappaB a good target for cancer therapy? Hopes and pitfalls, Nat. Rev. Drug Discovery 8 (2009) 33–40.
[27] T. Masaki, Y. Shiratori, W. Rengifo, et al., Cyclins and cyclin-dependent kinases: comparative study of hepatocellular carcinoma versus cirrhosis, Hepatology 37 (2003) 534–543.
[28] M. Suzui, M. Masuda, J.T. Lim, et al., Growth inhibition of human hepatoma cells by acyclic retinoid is associated with induction of p21(CIP1) and inhibition of expression of cyclin D1, Cancer Res. 62 (2002) 3997–4006.